RsaC sRNA modulates the oxidative stress response of Staphylococcus aureus during manganese starvation

David Lalaouna, Jessica Baude, Zongfu Wu, Arnaud Tomasini, Johana Chicher, Stefano Marzi, François Vandenesch, Pascale Romby, Isabelle Caldelari, Karen Moreau

Published online 28 August 2019

Nucleic Acids Research, 2019, Vol. 47, No. 18 ***9871–9887***
doi: 10.1093/nar/gkz728

RsaC sRNA modulates the oxidative stress response of *Staphylococcus aureus* during manganese starvation

David Lalaouna[1], Jessica Baude[2], Zongfu Wu[3], Arnaud Tomasini[1], Johana Chicher[4], Stefano Marzi[1], François Vandenesch[2,5], Pascale Romby[1], Isabelle Caldelari[1,*] and Karen Moreau[2,*]

[1]Université de Strasbourg, CNRS, Architecture et Réactivité de l'ARN, UPR9002, Strasbourg, France, [2]CIRI, Centre International de Recherche en Infectiologie, Inserm U1111, Université Lyon1, Ecole Normale Supérieure de Lyon, CNRS UMR5308, Lyon, France, [3]MOE Joint International Research Laboratory of Animal Health and Food Safety, College of Veterinary Medicine, Nanjing Agricultural University, Nanjing, China, [4]Plateforme protéomique Strasbourg-Esplanade, IBMC-CNRS, Strasbourg, France and [5]Centre National de Référence des Staphylocoques, Institut des Agents Infectieux, Hospices Civils de Lyon, Lyon, France

Received March 26, 2019; Revised July 22, 2019; Editorial Decision August 08, 2019; Accepted August 19, 2019

ABSTRACT

The human opportunistic pathogen *Staphylococcus aureus* produces numerous small regulatory RNAs (sRNAs) for which functions are still poorly understood. Here, we focused on an atypical and large sRNA called RsaC. Its length varies between different isolates due to the presence of repeated sequences at the 5 end while its 3 part is structurally independent and highly conserved. Using MS2-affinity purification coupled with RNA sequencing (MAPS) and quantitative differential proteomics, *sodA* mRNA was identified as a primary target of RsaC sRNA. SodA is a Mn-dependent superoxide dismutase involved in oxidative stress response. Remarkably, *rsaC* gene is co-transcribed with the major manganese ABC transporter MntABC and, consequently, RsaC is mainly produced in response to Mn starvation. This 3 UTR-derived sRNA is released from *mntABC*-RsaC precursor after cleavage by RNase III. The mature and stable form of RsaC inhibits the synthesis of the Mn-containing enzyme SodA synthesis and favors the oxidative stress response mediated by SodM, an alternative SOD enzyme using either Mn or Fe as co-factor. In addition, other putative targets of RsaC are involved in oxidative stress (ROS and NOS) and metal homeostasis (Fe and Zn). Consequently, RsaC may balance two interconnected defensive responses, i.e. oxidative stress and metal-dependent nutritional immunity.

INTRODUCTION

Staphylococcus aureus is a major human opportunistic pathogen responsible for a wide variety of infections, from superficial to deep-seated infections with high mortality (e.g. infective endocarditis, osteomyelitis and necrotizing pneumonia). Professional phagocytes (i.e. neutrophils and macrophages) represent the first line of host defence and are important components of innate immunity against *S. aureus* (1,2). After migration to the infection site, immune effectors deploy an arsenal of offensive and defensive strategies including phagocytosis, prevention of *S. aureus* dissemination by extracellular traps (ETs) (3), and synthesis of a battery of antimicrobial effectors such as reactive oxygen species (ROS) (1). ROS include superoxide anion ($O_2^{\cdot -}$), hydrogen peroxide (H_2O_2) and hydroxyl radical ($^{\cdot}OH$), which are also natural products of metabolism formed when oxygen becomes partially reduced during aerobic respiration (4). They have the potential to damage nucleic acids, proteins and lipids. Neutrophils also locally secrete the chelating agent calprotectin to sequester critical ions for bacterial growth such as manganese (Mn) and zinc (Zn) (5).

To evade immune defences and colonize numerous organs, *S. aureus* produces a wide range of virulence factors and stress-response proteins. They notably impede phagocytosis, escape ETs, extract nutrients from host cells and detoxify ROS (2,3). For example, superoxide dismutases (SOD) and catalases are produced to convert $O_2^{\cdot -}$ to H_2O_2, and then to water and oxygen (6). SODs are metalloenzymes classified according to their loaded cofactor: copper/zinc (Cu/Zn-SOD), manganese (Mn-SOD), nickel (Ni-SOD) or iron (Fe-SOD) (7). In *S. aureus*, two SODs

*To whom correspondence should be addressed. Tel: +33 388417068; Fax: +33 388602218; Email: i.caldelari@ibmc-cnrs.unistra.fr
Correspondence may also be addressed to Karen Moreau. Email: karen.moreau@univ-lyon1.fr

are involved in oxidative response (8,9). The major SOD enzyme SodA is strictly Mn-dependent while the cambialistic enzyme SodM is active when loaded with Mn or Fe and is therefore important in manganese limiting conditions (10). Remarkably, SodM is specific to *S. aureus* as coagulase-negative staphylococci lack *sodM* gene (9,10). There are conflicting reports regarding the role of SODs in virulence. An early study suggested no correlation between SOD activity and lethality in a mouse infection model (11). However, SOD activity was found higher in *S. aureus* strains isolated from infected patients (12). Deletion of *sodAM* reduced virulence in abscess or retro-orbital infection models (5,13). More recently, the contribution of each Sod enzyme was deciphered during mice infection (10). SodA plays a crucial role when Mn is abundant while SodM becomes the main enzyme assuring the resistance to oxidative stress when Mn is scarce. Nevertheless, the regulation of their synthesis is still poorly understood.

The production of *S. aureus* virulence factors is regulated by a combination of transcriptional regulators and regulatory RNAs (sRNAs) (14). Many sRNAs form base-pairings with their mRNA targets to control their expression and play key functions in adaptive processes and virulence (15). The most studied sRNA in *S. aureus* is RNAIII, one of the main intracellular effectors of the quorum sensing *agr* system. RNAIII represses the expression of virulence factors such as protein A, immunoglobulin-binding protein Sbi, coagulase, and of the repressor of toxins Rot while it activates the synthesis of hemolysin α (16–21). In this study, we have analyzed the function of another very peculiar and large sRNA, named RsaC, which was found highly expressed in acute osteomyelitis, a bone infection usually caused by *S. aureus* (22). Here, we identified *sodA* mRNA as a primary target of the 3 -UTR derived sRNA RsaC, which is mainly produced upon Mn starvation. By repressing the translation of the Mn-containing enzyme SodA, RsaC avoids the synthesis of a non-functional enzyme. Concurrently, RsaC indirectly enhances the oxidative stress response mediated by the cambialistic enzyme SodM, which in absence of manganese, uses Fe as a cofactor to restore the ROS detoxification pathway. We also demonstrated that RsaC might have a broader role in oxidative stress response (ROS and NOS) and in metal homeostasis (Mn, Fe and Zn). The consequences of this regulation on *S. aureus* pathogenicity will be discussed.

MATERIALS AND METHODS

Strains, plasmids and growth conditions

Staphylococcus aureus strains and plasmids used in this study are listed in Supplementary Table S1. *Escherichia coli* strain DH5α (Promega) was used as host strain for plasmid constructions. *Staphylococcus aureus* strain RN4220 (23) or *E. strain* DC10B (24) were used as host strains for plasmid amplification before electroporation in *S. aureus* HG001. Transformation of *E. coli* DH5α or DC10B was performed by heat shock and *S. aureus* strains were transformed by electroporation (Bio-Rad gene Pulser).

Escherichia coli strains were cultivated in lysogeny broth (LB). *Staphylococcus aureus* strains were isolated on glucose peptone (GP), tryptic soy (TS) or blood agar plates. Overnight cultures in brain-heart infusion (BHI) or in tryptic soy broth (TSB) ± erythromycin (5 μg/ml) were diluted 50-fold in fresh medium and grown at 37°C (180 rpm, 5:1 flask-to-medium ratio). To induce Mn starvation, cells were grown in BHI-chelex medium as followed. We added 5% Chelex-100 resin (Sigma) to BHI medium and mix 6h at 20°C. The medium was sterile filtered and, according to Kehl-Fie *et al.* (25), we complemented it with metal ions at the following concentrations: 100 μM $CaCl_2$, 25 μM $ZnCl_2$, 1 mM $MgCl_2$, 1 μM $FeSO_4$. As a control, BHI-chelex medium was also supplemented with 25 μM $MnCl_2$.

Deletion of $rsaC_{1116}$ gene (*rsaC*) in HG001 strain was performed using pMAD (26). Chromosomal regions upstream and downstream of the *rsaC* sequence were amplified by PCR (RsaC-PCR1-Rev/RsaC-PCR1-For and RsaC-PCR2-Rev/RsaC-PCR2-For, respectively) (Supplementary Table S2) and then cloned into pMAD vector. The resulting plasmid (pLUG1110) was electroporated into RN4220 recipient strain and then transferred to HG001. Growth at non-permissive temperature (44°C) was followed by several subcultures at 30°C and 37°C to favor double crossing over as previously described (26). As control, we verified that deletion of *rsaC* does not alter the expression of surrounding genes. Indeed, *rsaC* gene is located between *mntC* and *nhaK*_1 genes, which encodes a subunit of a manganese ABC transporter and a proton pump, respectively (Supplementary Figure S1A). Using qRT-PCR experiments, we have verified that no difference existed in the expression level of downstream and upstream genes between wild type and mutant strains (Supplementary Figure S1B). To complement *rsaC* strain (*rsaC*+), $rsaC_{1116}$ gene was amplified using *Pst*I-$RsaC_{1116}$-For/*BamH*I-$RsaC_{1116}$-Rev oligonucleotides (Supplementary Table S2). The amplicon $RsaC_{1116}$ was digested by *Pst*I and *BamH*I restriction enzymes and inserted into a *Pst*I/*BamH*I digested pCN51-P3 plasmid. The quorum sensing-dependent P3 promoter allows an overexpression of the downstream gene in stationary phase of growth. To generate the $RsaC_{1116}$mut construct (deletion of nucleotides +1000 to +1006), two independent PCR reactions were performed with the following oligonucleotides: *Pst*I-$RsaC_{1116}$-For/RsaCmut-Rv and RsaCmut-For/*BamH*I-RsaC-Rev. The two PCR products were then mixed to serve as template for a third PCR (*Pst*I-$RsaC_{1116}$-For/*BamH*I-$RsaC_{1116}$-Rev). The amplicon $RsaC_{1116}$mut was digested by *Pst*I and *BamH*I restriction enzymes and inserted into a *Pst*I/*BamH*I digested pCN51-P3 plasmid. To obtain a pJET-T7-*sodA*, a PCR fragment was amplified using oligos T7-*sodA*-For/T7-*sodA*-Rev (Supplementary Table S2) and then cloned into pJET1.2/blunt vector (ThermoFisher). For MAPS experiment, MS2 aptamer was fused to the 5 end of $RsaC_{544}$ using oligonucleotides PstI-MS2-RsaC-For and *BamH*I-RsaC-Rev (Supplementary Table S2). Obtained fragment was cloned into *Pst*I/*BamH*I-digested pCN51-P3. Total DNA and plasmid DNA were prepared using DNAeasy tissue Kit and Qiaprep Miniprep respectively (Qiagen).

Northern blot analysis

Total RNAs were prepared from different volumes of *S. aureus* cultures taken at 2 h (OD_{600nm}∼0.4; 15 ml), 4 h

($OD_{600\,nm}$ ~2.5; 10 ml) and 6 h ($OD_{600\,nm}$ ~5; 5 ml). After centrifugation, bacterial pellets were resuspended in RNA Pro Solution (MP Biomedicals). Lysis was performed with FastPrep apparatus (MP Biomedicals). RNA purification followed strictly the procedure described for the FastRNA Pro Blue Kit (MP Biomedicals).

Electrophoresis of total RNA (10–20 μg) was performed on 1% agarose gel containing 25 mM guanidium thiocyanate. After migration, RNAs were vacuum transferred on Hybond N+ nitrocellulose membrane (GE Healthcare Life Sciences). Hybridization with specific digoxygenin (DIG)-labelled probe complementary to RsaC or 5S sequence followed by luminescent detection were carried out as described previously (16). For *mntA*, we used a radiolabelled DNA probe (Supplementary Table S2). The labeling of the 5 end of the oligonucleotide was performed with T4 polynucleotide kinase (Fermentas) and [γ^{32}P] ATP. For determination of molecular weights, we used the Dynamarker® Prestain Marker for RNA high (CliniSciences).

MS2-affinity purification coupled with RNA sequencing (MAPS)

The MS2 aptamer, which is recognized by the MS2 coat protein, was fused to the 5 end of $RsaC_{544}$. Here, we used a shorter form of RsaC due to nonspecific interaction of $RsaC_{1116}$ with the affinity column. $RsaC_{544}$ construct carries the whole 3 domain of RsaC (447 nt) and 97 nucleotides from the 5 part, which enables to preserve the secondary structure of the 3 domain of RsaC (Figure 1B). This construct was expressed *in vivo* under the control of the quorum sensing-dependent promoter P3 and confirmed as functional when compared to the full-length $RsaC_{1116}$ and MS2-$RsaC_{1116}$ (Supplementary Figure S2). Indeed, the overexpression of the three RNAs induces similar ROS accumulation, revealing that the 3 domain of RsaC is sufficient to modulate the oxidative stress response.

Crude extracts from *rsaC* strain expressing MS2-$RsaC_{544}$ or from WT strain expressing MS2 tag alone (control) were harvested after 6 h of growth at 37°C in BHI medium. MS2-affinity purifications were performed as previously described (27,28). All steps were performed at 4°C. Poly-Prep chromatography column (Biorad) containing amylose resin (300 μl; NEB) were washed three times with 10 ml of Buffer A (20 mM Tris–HCl pH 8, 150 mM KCl, 1 mM $MgCl_2$, 1 mM DTT), before addition of 3600 pmol of MS2-MBP. Crude bacterial extracts (4 ml) were directly loaded, followed by three washes with 10 ml of Buffer A. Finally, RNAs were eluted from the column with 1 ml of Buffer E (20 mM Tris–HCl pH 8, 150 mM KCl, 1 mM $MgCl_2$, 1 mM DTT, 0,1% Triton X-100, 12 mM maltose). Eluted RNAs were extracted with phenol:chloroform:isoamylalcohol (25:24:1 (v/v), Roth) and precipitated with 3 volumes of cold absolute ethanol in the presence of 0.3 M sodium acetate. RNA samples were then treated with DNase I prior to RNA-seq analysis. MS2-affinity purifications were performed in duplicates.

RNA quality and quantity assessments were performed on Agilent Nano Chip on Bioanalyzer 2100. RNA samples were ribo-depleted (Ribo-Zero rRNA Removal Kit (Bacteria) Illumina) and cDNA libraries were prepared using the Random Hexamer approach and sequenced by Fasteris (Switzerland). Libraries were sequenced using Hi-Seq 2500 system (Illumina). RNA-seq analysis was performed according to Lalaouna et al. (2018) (27). Reads were processed and aligned on HG001 genome (29) using the Galaxy platform (30). We used DEseq2 to estimate enrichment values for MAPS ($n = 2$) (P-value < 0.05; Fold change (FC) > 2) (Table 1). The whole list of RNA enriched with MS2-$RsaC_{544}$ is available in Supplementary Table S3. MAPS data that support our findings are available in the GEO database with the accession code GSE128741.

Differential proteomic analysis on cytoplasmic proteins

Label free spectral count analysis was performed in triplicate on cytoplasmic proteins extracts prepared from tested strains using nanoLC–MS/MS. Cells were harvested after 6 h of growth in BHI (Supplementary Table S4) or in BHI-chelex supplemented or not with 25 μM of $MnCl_2$ (Supplementary Table S5). Proteins were extracted from cytoplasm of tested strains and were digested with sequencing-grade trypsin (Promega, Fitchburg, MA, USA) as previously described (28). The samples were analyzed by nanoLC-MS/MS either on a NanoLC-2DPlus system (with nanoFlex ChiP module; Eksigent, Sciex, Concord) coupled to a TripleTOF 5600 mass spectrometer (AB Sciex) or on a QExactive+ mass spectrometer coupled to an EASY-nanoLC-1000 (Thermo-Fisher Scientific, USA). Data were searched against *S. aureus* HG001 database using Mascot algorithm (version 2.5, Matrix Science, London, UK) through ProlineStudio 1.4 package (http://proline.profiproteomic.fr/). Peptides were validated on Mascot pretty rank equal to 1, an ion score cut-off equal to 25, and 1% FDR on both peptide spectrum matches (PSM) and protein sets (false discovery rate-based ion score). The total number of spectra was recorded for all the proteins, allowing to quantify these proteins across all the samples (quantification by spectral count). Data were submitted to a negative-binomial test using an edgeR GLM regression through R (R v3.5.0), normalized according to a median-to-ratio method to calculate fold changes (FC) and P-values. The mass spectrometric data that support our findings are available via ProteomeXchange with identifier PXD013225.

Preparation of RNAs for *in vitro* experiments

PCR fragments containing T7-$RsaC_{544}$, T7-$RsaC_{544}$mut, T7-*ldh1* (from –167 to +418), T7-*rex* (from –103 to +205), T7-*sarA* (full-length; from –147 to +375), T7-*sodM* (full-length; from –28 to +651), T7-*sufC* (full-length; from –100 to +762), T7-*sufD* (from –97 to +626), T7-*znuB* (full-length; from –60 to +786), T7-*znuC* (from –22 to +646) and T7-*zur* (full-length; from –212 to 412) were used for *in vitro* transcription with T7 RNA polymerase (Supplementary Table S2). We used HG001 genomic DNA as DNA template for most constructs. For T7-$RsaC_{544}$ and T7-$RsaC_{544}$mut, we used pCN51-P3-MS2-$RsaC_{544}$ and pCN51-P3-$RsaC_{1116}$mut, respectively. The transcription of full-length mRNA *sodA* was performed from a *Dra*I/*Xho*I-digested pJET-T7-*sodA* plasmid (from –28 to +600). RNAs

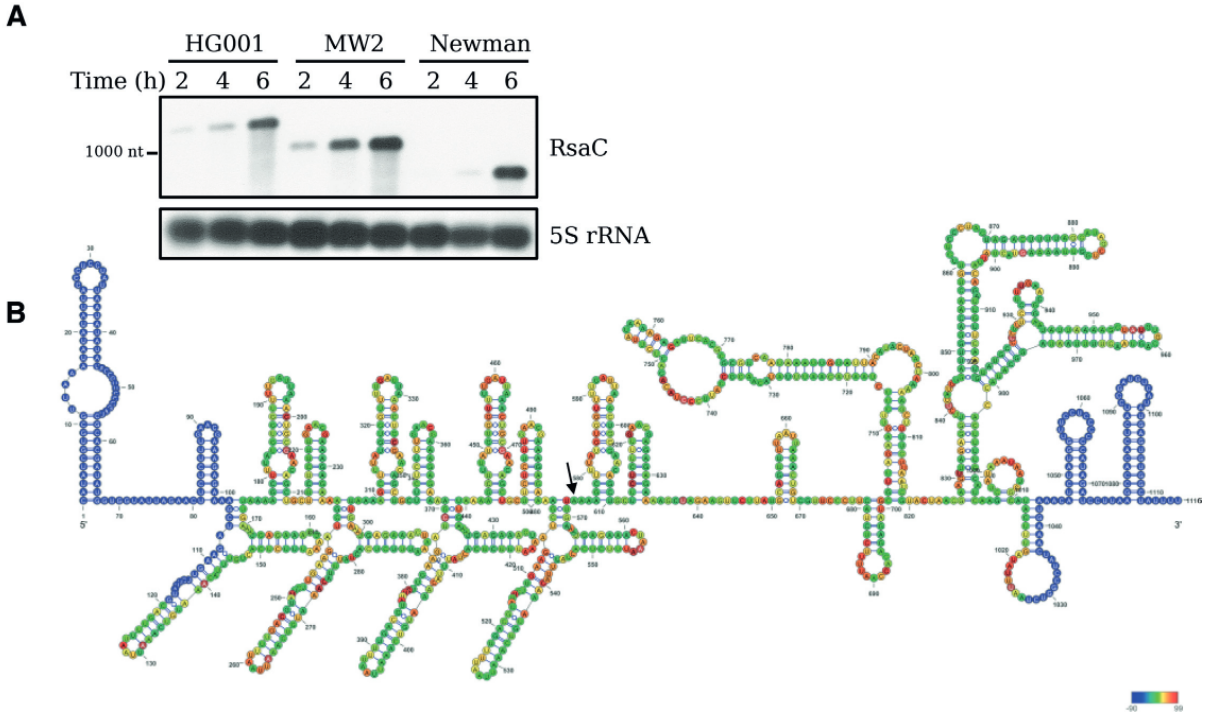

Figure 1. RsaC is a large and highly structured sRNA. (**A**) Northern blot analysis of RsaC sRNA in three different *S. aureus* strains (HG001, MW2 and Newman). Total RNA was extracted after 2, 4 and 6 h of growth in BHI at 37°C. 5S rRNA was used as loading control. Data are representative of three independent experiments. (**B**) Secondary structure model of RsaC. The structure of RsaC (from HG001 strain) was mapped using selective 2 -hydroxyl acylation by benzol cyanide and the reactivity was analyzed by primer extension (SHAPE). Data were analyzed, and each modification was quantified using QuSHAPE software. The secondary structure was drawn using RNA structure and VARNA considering the reactivity of each ribose. The regions, which were not mapped, are shown in blue. The color code for each reactivity is given on the right side of the secondary structure model, red is for the highest reactivity while green is for the lowest reactivity. A black arrow indicates the +1 of $RsaC_{544}$.

were then purified using a 6% polyacrylamide–8 M urea gel electrophoresis. After overnight elution in Elution Buffer (0.5 M ammonium acetate pH 6.5, 1 mM EDTA and 0.1% SDS), RNAs were precipitated in cold absolute ethanol and washed with 80% ethanol. RNAs were dephosphorylated using Fast AP (ThermoFisher), according to the manufacturer protocol. The labeling of the 5 end of dephosphorylated RNA was performed with T4 polynucleotide kinase (Fermentas) and [γ^{32}P] ATP as previously described (16).

Gel retardation assays

5 -radiolabeled $RsaC_{544}$ (15000 cpm/sample, concentration <1 pM) and cold mRNAs were renaturated separately by incubation at 90°C for 1 min in Buffer GR- (20 mM Tris–HCl pH 7.5, 60 mM KCl, 40 mM NH_4Cl, 3 mM DTT), cooled 1 min on ice, and incubated 15 min at RT in presence of 10 mM $MgCl_2$. For each experiment, increasing concentrations of cold mRNA were added to the 5 end labelled $RsaC_{544}$ in a total volume of 10 µl containing Buffer GR+ (20 mM Tris–HCl pH 7.5, 60 mM KCl, 40 mM NH_4Cl, 3 mM DTT, 10 mM $MgCl_2$). Complex formation was performed at 37°C during 15 min. After incubation, 10 µl of glycerol blue was added and samples were loaded on a 6% polyacrylamide gel containing 10 mM $MgCl_2$ under non-denaturing conditions (8 h, 300 V, 4°C). Quantification of data corresponding to $RsaC_{544}$ and to $RsaC_{544}$/mRNA complex was done with ImageQuant TL software (GE Healthcare Life Sciences). Under these conditions where the concentration of the labeled RNA is negligible, the Kd dissociation constant can be evaluated as the concentration of the cold RNA that showed 50% of binding. The same protocol was used with 5 -radiolabeled $RsaC_{544}$mut.

Toe-printing assays

The preparation of *S. aureus* 30S ribosomal subunits, the formation of a simplified translational initiation complex (constituted by *S. aureus* 30S ribosomal subunit, initiator $tRNA^{fMet}$ and *sodA* mRNA), and the extension inhibition conditions were performed as described previously (31). Increasing concentrations of $RsaC_{544}$ (25–400 nM) were used to monitor their effects on the formation of the initiation complex (250 nM of 30S *S. aureus*; 4 µM of $tRNA^{fMet}$) with *sodA* mRNA (50 nM).

Primer extension assays

Primer extension assays were performed using 30 µg of total RNA, incubated with 5 -radiolabeled oligonucleotide (PE-RsaC-Rev, Supplementary Table S2), 2.5 mM dNTPs and AMV reverse transcriptase (4 units, NEB). RNA template was removed by addition of 3 µl of 3 M KOH and 20 µl

Table 1. List of RNAs significantly co-purified with MS2-RsaC$_{544}$

ID	Gene name	Function	Fold change MS2-RsaC/Ctrl	*P*-value
HG001_00569	-	RsaC sRNA	9.981	3.33E-23
HG001_01477	*sodA*	Superoxide dismutase SodA	8.088	2.44E-18
HG001_01627	*gloB_1*	Hydroxyacylglutathione hydrolase	5.406	4.20E-13
HG001_02152	*fba*	Fructose-bisphosphate aldolase	4.082	4.84E-10
HG001_00556	*sarA*	Transcriptional regulator SarA	3.156	1.88E-06
HG001_00934	*ptsI*	Phosphoenolpyruvate-protein phosphotransferase	3.122	5.80E-07
HG001_00252	-	FtsX-like permease family protein	3.093	5.72E-07
HG001_02633	*envR*	DNA-binding transcriptional regulator EnvR	2.877	7.08E-06
HG001_00671	*fecD_1*	Fe(3+) dicitrate transport system permease protein FecD	2.721	4.27E-05
HG001_00933	*ptsH*	Phosphocarrier protein HPr	2.692	1.30E-05
HG001_01479	*znuB*	High-affinity zinc uptake system membrane protein ZnuB	2.642	4.16E-05
HG001_00967	-	Cysteine-rich secretory protein family protein	2.613	2.67E-05
HG001_01416	*srrB*	Sensor protein SrrB	2.576	2.71E-05
HG001_02376	-	Hypothetical protein	2.491	8.80E-05
HG001_01478	*zur*	Zinc-specific metallo-regulatory protein Zur	2.446	0.000206
HG001_01220	*msrR*	Regulatory protein MsrR	2.443	9.65E-05
HG001_01721	*menE*	2-succinylbenzoate–CoA ligase	2.351	0.000382
HG001_02519	-	Hypothetical protein	2.222	0.000486
HG001_00968	-	Hypothetical protein	2.21	0.000569
HG001_01480	*znuC*	High-affinity zinc uptake system ATP-binding protein ZnuC	2.176	0.001228
HG001_02411	-	hypothetical protein	2.146	0.001107
HG001_01710	*yvgN*	Glyoxal reductase	2.124	0.001455
HG001_01657	*ccpA*	Catabolite control protein A	2.101	0.001521
HG001_00540	*ywqN_2*	Putative NAD(P)H-dependent FMN-containing oxidoreductase YwqN	2.065	0.001444
HG001_01626	*nhaX*	Stress response protein NhaX	2.056	0.001481
HG001_01845	*lytN_3*	putative cell wall hydrolase LytN precursor	2.056	0.001999
HG001_01925	*cobQ*	Cobyric acid synthase	2.035	0.002683
HG001_00932	-	Hypothetical protein	2.029	0.001941
HG001_02069	*rex*	Redox-sensing transcriptional repressor Rex	2.023	0.001773
HG001_00568	*nhaK_1*	Sodium, potassium, lithium and rubidium/H(+) antiporter	2.005	0.002142
HG001_02589	-	Virus attachment protein p12 family protein	2.002	0.004538

of Destroy Buffer (50 mM Tris–HCl pH 8.0, 0.5% SDS, 7.5 mM EDTA) for 3 min at 90°C, followed by 1 h at 37°C. Samples were finally precipitated and migrated on a denaturing 10% polyacrylamide gel, next to sequencing ladder. The sequencing ladder was obtained with a DNA template (PCR with oligonucleotides PE-RsaC-For and PE-RsaC-Rev, from genomic DNA). Here, ddNTP were added to stop the reaction performed by the Vent (exo-) DNA polymerase (2 units, NEB). As an example, the A reaction is composed of 0.25 mM ddATP, 0.025 mM dATP, 0.05 mM dGTP, 0.05 mM dCTP and 0.05 mM dTTP. 0.1% Triton was also added to the reaction. PCR was performed as follows: 1 min at 95°C, 1 min at 52°C and 1 min at 72°C (25 cycles). The primer PE-RsaC-Rev is located at nucleotides +42 to +59 (from the +1 of RsaC).

Footprinting assays

RsaC$_{544}$-*sodA* mRNA complex formation was carried out at 37°C for 15 min in Native Buffer (20 mM Tris–HCl pH 7.5, 10 mM $MgCl_2$ and 150 mM KCl). Enzymatic hydrolysis was performed on the unlabelled and renatured RsaC sRNA (50 nM) in absence or in presence of *sodA* mRNA (75, 150 or 300 nM). The reaction was performed in Native Buffer with RNase V1 (0.5 U) or with RNase T2 (0.05 U) at 20°C for 5 min in presence of 1 μg of total tRNA. The reactions were stopped by phenol extraction followed by RNA precipitation. The enzymatic cleavages in RsaC were detected by primer extension with AMV reverse transcriptase according to Fechter *et al.* (32).

Determination of RNA structure with SHAPE

To elucidate the secondary structure of RsaC sRNA, SHAPE reactivity assays were performed as previously described by Rice *et al.* (2014) (33). RNA folding was probed with benzoyl cyanide (BzCN), which modified 2 -hydroxyl of riboses. 1 pmol of RNA was denatured and renatured in SHAPE-BzCN buffer with 2 μg of yeast tRNA. Then, BzCN was added with different final concentrations (10-50-150 mM). After 1 min at 20°C, RNA was precipitated. Thereafter, reverse transcription was performed with VIC-labelled oligonucleotides (Supplementary Table S2). In parallel, ddGTP sequencing of 1 pmole RNA was made with the same oligonucleotide labelled with NED fluorophore. cDNA samples were analysed by capillary electrophoresis and data processed by QuSHAPE software (34). SHAPE data (Supplementary Table S6) were used to constrain structure prediction by RNAstructure (35). The secondary structure of RsaC was finally visualized using VARNA (36) (Figure 1B).

RT-PCR

RT-PCR was performed using OneStep RT-PCR Kit (Qiagen) according to the manufacturer's instructions. Total RNA extracted after 4 or 6 h of growth in BHI medium was used as template (after DNase I treatment). Primers are described in Supplementary Table S2. The same experiment was performed without RT enzyme as a control.

Determination of the 5 end status of RsaC

To determine if the 5 end of RsaC is mono- or tri-phosphorylated, we used Terminator™ 5 -Phosphate-Dependent Exonuclease Terminator (Epicentre) according to manufacturer's protocol. Total RNA (10 μg) was incubated with Terminator Exonuclease (1U) and Terminator 1X Reaction Buffer A at 30°C for 1 h. Subsequently, we performed phenol extraction and ethanol precipitation. Northern blot analysis was performed on 1% agarose gel containing 25 mM guanidium thiocyanate.

Superoxide stress assays

Sensitivity to methyl viologen (MV) was assessed by viability test (13). Fresh BHI broth was inoculated with an overnight culture to an initial OD_{600nm} of 0.05 and cultivated at 37°C with shaking (200 rpm). Cells were challenged with MV (10 mM) in early-exponential phase (2 h). Samples were collected at appropriate intervals post-challenge. Viability of bacteria was determined by plating onto GP agar supplemented with 5 μg/ml erythromycin. Experiments were performed in triplicate.

SOD activity assays

SOD activity assays were performed as previously described (37). Basically, when exposed to light, riboflavin produces $O_2^{\cdot -}$, which reduces tetrazolium to the dark blue formazan dye. The presence of SOD enzymes hinders this reaction and can be visualized by an achromatic area (negative staining). Samples were collected after 8 h of growth in absence or presence of methyl viologen (10 mM; BHI) or after 6h in BHI-chelex ±25 μM $MnCl_2$. Cells were then washed in PBS and lysed (8). Total protein concentration was determined by Bradford assay (Bio-Rad). SodA and SodM activities were determined by negative staining on native polyacrylamide gel (9). Equal amounts of protein (20 μg) were resolved on 12% polyacrylamide gels by electrophoresis in glycine buffer without sodium dodecyl sulfate. After the run, the gel was soaked in 1.225 mM of nitro blue tetrazolium (NBT) solution for 45 min and then washed with sterile distilled water. Subsequently, the gel was soaked in a solution containing 0.028 mM riboflavin and 28 mM TEMED (tetramethylethylene diamine) for another 45 min. The gel was exposed to light to initiate the photochemical reaction. The SOD activity was monitored as a clear zone surrounded by a dark blue background.

Endogenous ROS production

Cells were harvested (1 ml at OD_{600nm} = 1) after 6h of growth and washed twice with PBS. The probe 2 ,7 -dichlorofluorescein diacetate (Sigma) was then added to cell suspensions to a final concentration of 10 μM. Fluorescence intensity (FI) was acquired during 5 h using 96-well spectrofluorimeter (Ex/Em = 485/538 nm). The FI value was normalized to the $OD_{600\ nm}$ of each culture. The experiment was performed in triplicate.

RESULTS

RsaC is a long and structured RNA whose length varies between isolates

We first analyzed by Northern blot the expression of RsaC in three different strains (HG001, MW2 and Newman) during growth in BHI at 37°C (Figure 1A). RsaC is mainly produced in stationary phase and its length varies depending on tested strains. To understand this variation, the 5 end of the longest form of RsaC sRNA (in HG001) was mapped using primer extension. The experiment shows a RT stop corresponding to a fragment with a length of 1116 nt (Supplementary Figure S3).

By performing a comparative multiple sequence alignment with MW2 and Newman strains, we observed that the 3 domain of RsaC (comprising 447 nt) is highly conserved (>95%) (Supplementary Figure S4A), while its 5 domain differs in strains due to variation in the number of repeats (from 2 to 4; 133 nt) (Supplementary Figure S4B). A truncated repeat of 58 nt marks the end of the 5 part of RsaC. Therefore, RsaC is 850 nt-long (2 repeats) in Newman, 984 nt-long (3 repeats) in MW2 and 1116 nt-long (longest form; four repeats) in HG001. We expanded our analysis to all bacterial genomes using a sequence similarity search program (BLASTn; Supplementary Table S7) and observed that RsaC is restricted to *S. aureus* and the closely related *S. argenteus* species. The length of RsaC sRNA is ranging from 584 nt (a single truncated repeat) to 1116 nt (four repeats and a truncated repeat). This highlights the wide variability in length and composition of the 5 part of RsaC.

We probed the secondary structure of RsaC (from HG001 strain) using selective 2 -hydroxyl acylation of riboses with benzoyl cyanide (BzCN) (33). Resulting 2 -*O*-adducts were detected by primer extension and data were analysed and quantified using QuSHAPE software (34). The BzCN reactivity (Supplementary Table S6) provides information on the local nucleotide flexibility and the highest reactivities of riboses are indeed mainly located in unpaired regions. The proposed secondary structure model, which takes into account the ribose reactivities, shows that RsaC is a highly structured sRNA characterized by two large and independent domains (Figure 1B). The 5 part is constituted of four repeat motifs, each of them carrying four distinct well-characterized stem-loop structures. The region from nucleotides +920 to +1070 was also probed with various ribonucleases specific either for unpaired nucleotides (RNase T2) or for double-stranded regions (RNase V1). These data support the proposed secondary structure model since the RNase T2 cleavages were preferentially located in the apical loops while major RNase V1 cuts occurred in paired regions (Figure 2D). The 3 part of RsaC is characterized by two large hairpin structures interrupted by internal loops and by several interhelical unpaired regions (Figure 1B).

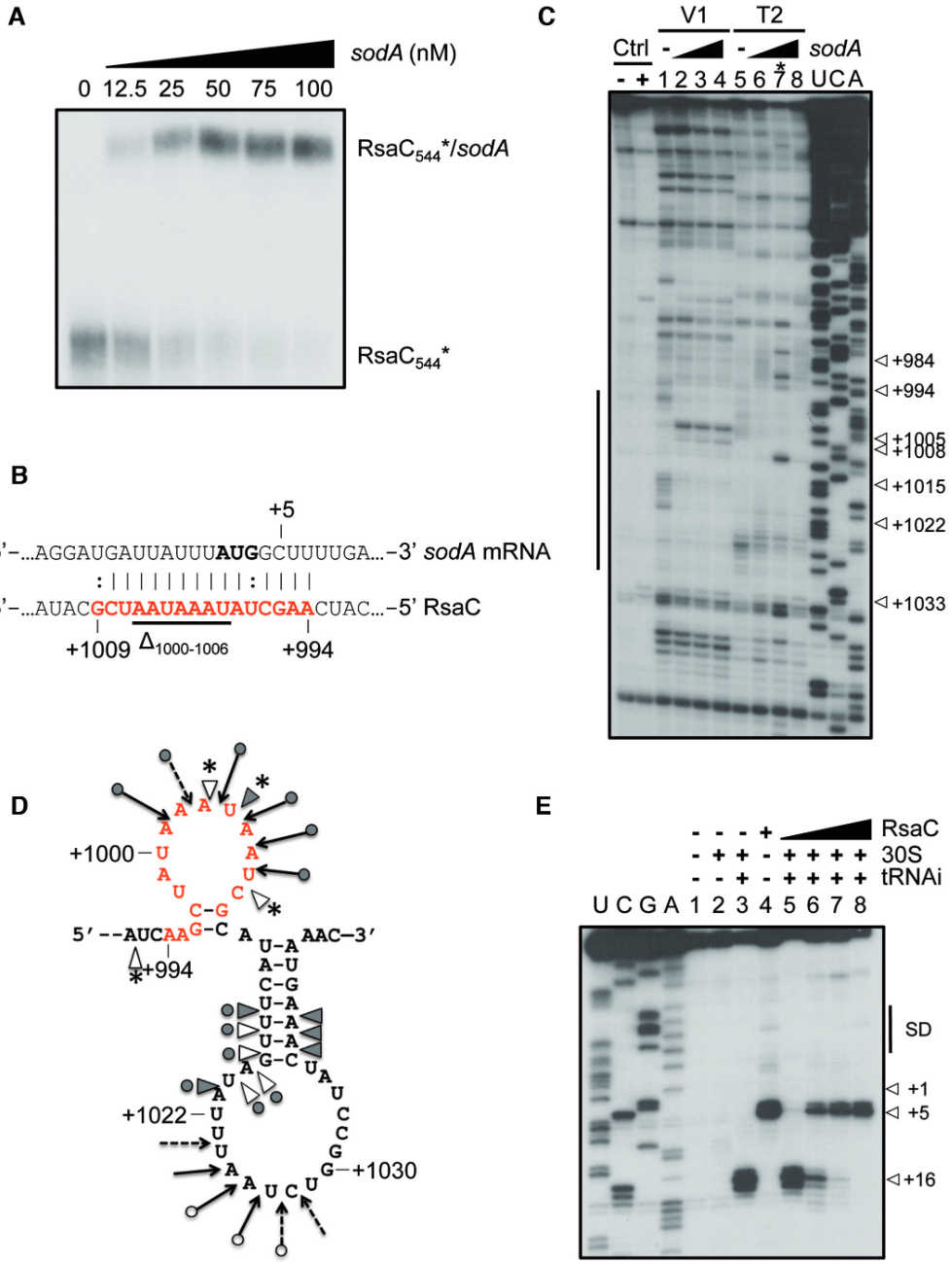

Figure 2. RsaC binds to *sodA* mRNA and blocks its translation. (**A**) Gel retardation assays using $RsaC_{544}$ sRNA and full-length *sodA* mRNA. 5 end-radiolabeled $RsaC_{544}$ (*) was incubated with increasing concentrations of *sodA* mRNA (from 0 to 100 nM). (**B**) The RsaC:*sodA* pairing site predicted using IntaRNA software is indicated in red. The AUG start codon is in bold. Deleted nucleotides ($\Delta_{1000–1006}$) in RsaCmut sequence are underlined. (**C**) Footprint of *sodA* mRNA on RsaC. Incubation controls (Ctrl) were performed in absence of RNases on RsaC either free (–) or bound to *sodA* (50 nM, +). Reactions with either RNase V1 (V1) or RNase T2 (T2) were performed with RsaC (50 nM) in absence (lanes 1 and 5) or in presence of increasing concentrations of *sodA* mRNA (lanes 2–4 and 6–8; 75, 150 or 300 nM, respectively). U, C, A: sequencing ladders. *Lane 7 should not be considered due to a technical glitch. On the left side, a bar denotes changes in cleavages as the result of *sodA* binding. (**D**) Schematic representation of *sodA* pairing site on RsaC sRNA revealed by footprinting assays. RNase V1 cleavages are denoted by grey triangles for strong cut and empty triangles for moderate cut. RNase T2 cleavages are shown by filled arrows for strong cut and dashed arrows for weak cut. New RNase V1 cleavages are labelled by stars. The predicted pairing site by IntaRNA software is indicated in red. (**E**) Toe-printing assay monitoring the effect of RsaC on the formation of the ternary ribosomal initiation complex comprising *S. aureus* 30S subunit, initiator $tRNA^{fMet}$ and *sodA* mRNA (50 nM). Lanes 1–4: incubation controls (lane 1: *sodA* mRNA alone; lane 2: *sodA* mRNA with 30S subunit; lane 3: *sodA* mRNA with 30S subunit and initiator $tRNA^{fMet}$ (tRNAi); lane 4: *sodA* mRNA with RsaC); lanes 5–8: formation of the initiation complex in presence of increasing concentrations of RsaC (25, 50, 100, 400 nM). U, C, G, A: sequencing ladders; SD: Shine-Dalgarno sequence; +1: start codon; +5: RT stop induced by RsaC binding; +16: toe-printing signal. Data are representative of two independent experiments.